Double-electron capture as a two-step process

M. S. Gravielle and J. E. Miraglia
Instituto de Astronomía y Física del Espacio, Consejo Nacional de Investigaciones Científicas y Técnicas, 1428 Buenos Aires, Argentina
(Received 6 May 1991)

Double-electron capture by the impact of heavy projectiles on heliumlike atoms is studied with a two-electron model. The process is here considered a two-step collision, which in the frame of the distorted-wave formalism is related to the second order. This second order is evaluated by using an on-shell Green function representing one electron in each center, and it is found to be related, after some approximations, to the independent-electron model. In particular, the exact impulse approximation is used to calculate the single-capture T-matrix elements, and the electronic repulsion is included as a dynamic perturbation in first order. A configuration-interaction wave function is employed to describe the ground state of helium for double capture $1s^2 \rightarrow 1s^2$ in a He^{2+}-He collision. For this benchmark, differences with the use of a Hartree-Fock wave function instead are found to be negligible. Thereafter, capture to single excited states for the same system is calculated by using Hartree-Fock and variational electronic wave functions. Also, double capture for multiply charged ions on helium is calculated. Differential cross sections for double-capture He^{2+}-He collisions at 60 keV/amu impact energy are presented and compared with previous experiments. The present theory produces good agreement with the available data.

PACS number(s): 34.70.+e

I. INTRODUCTION

Multiple-electron capture is a very interesting process for the study of the dynamics of a multiple-electron system during a collision. State-selective experiments at high energies are difficult [1], and the corresponding theory faces the nontrivial task of dealing with various active electrons. To treat such systems, the independent-electron model (IEM) is generally assumed. Thus, the n-particle system is decomposed in a collection of independent clusters of three particles (the projectile P, the nucleus target T, and one electron e), which are solved with an appropriate theoretical technique. Neither momentum nor energy can be transferred from one cluster to another. Relaxation is not allowed, and correlation is dropped, so they evolve independently from each other. A formal derivation of this model was worked out by McGuire and Weaver [2]. The IEM has certainly proved to be successful to deal with single capture induced by fast ions [3]. For double processes, the IEM leads to the product of single probabilities, which has been largely used to calculate double capture within the quantum [4–7] and classical formalisms [8,9].

There is an improvement that considers the electronic correlation in the bound states, for example, through the use of the Pluvinage wave functions [10]. This model, sometimes called the independent-event model [10], still uses the product of probabilities.

Few attempts have been made to solve the two-electron Schrödinger equation via a basis expansion within the semiclassical coupled channels. In the intermediate-energy range (including translation factors) two types of expansions of the time-dependent total wave function were investigated, namely the Slater- [11,12] and Gauss-type orbitals [13]. The success of these methods is generally restrained to the intermediate-energy range, unless the basis includes the continuum as an intermediate state.

In the present paper, we have studied double capture with a two-electron distorted-wave formalism. In this frame, the first order represents a single-step collision; it has been found [10] to be much smaller than the second one, and it was dropped here. Therefore, we have only concentrated on the second order, which involves a two-step process. It is calculated by using an on-shell propagator representing one electron in the target and the other one in the projectile. In this way, double capture may be seen as two subsequent single-capture processes, which, after several approximations, leads to the IEM.

In Sec. II, we present the general theory, and in Sec. III the exact-impulse approximation (IA) is used to evaluate the single-capture T-matrix elements. We have described the bound states, a lineal combination of products of two one-particle orbitals, which can be coming from configuration-interaction (CI), Hartree-Fock (HF), or variational electronic wave functions. The electronic repulsion has been included in first order as a perturbation potential during the collision, and relaxation has also been considered. In Secs. IV A and IV B total cross sections for the symmetric case $He^{2+}+He(1s^2) \rightarrow He(1s^2, 1s2s, 1s2p)+He^{2+}$ are obtained and compared with experiments and other theoretical results. In Sec. IV C we present results for the asymmetric systems $X^{Z+}+He(1s^2) \rightarrow X^{(Z-2)+}(1s^2)+He^{2+}$, $Z=3,5$. In Sec. V we show differential cross sections for the symmetric case. Throughout the work the internuclear interaction will be dropped and reintroduced through the well-known Coulomb phase factor when calculating the differential cross section. Atomic units are used, except where indicated.

II. THEORY

Let us assume a collision of a structureless projectile P (of mass M_P and charge Z_P) with a heliumlike atom composed of a target nucleus (M_T and Z_T) and two electrons (e_1 and e_2). Coordinate systems are shown in Fig. 1, and the corresponding transformations are listed in the Appendix. Reduced masses ν_X, μ_{X1}, and μ_{X2} are associated with the coordinates $\mathbf{R}_X$, $\mathbf{r}_{X1}$, and $\mathbf{r}_{X2}$ (with $X=T$ or P), respectively, and ν is associated with the coordinate $\mathbf{R}$. The potential V_{Xj} is the Coulomb potential between the nucleus X and the electron j ($j=1,2$), and $V_{12}=1/r_{12}$ is the electronic repulsion.

The total Hamiltonian H reads

$$H=-\frac{1}{2\nu_T}\nabla^2_{\mathbf{R}_T}+H_T+V_{P1}+V_{P2}\ , \tag{2.1}$$

where H_T is the atomic Hamiltonian:

$$H_T=-\frac{1}{2\mu_{T1}}\nabla^2_{\mathbf{r}_{T1}}-\frac{1}{2\mu_{T2}}\nabla^2_{r_{T2}}+V_{T1}+V_{T2}+V_{12}\ . \tag{2.2}$$

In the distorted-wave formalism the exact T-matrix element is $T_{fi}=T^{(1)}_{fi}+T^{(2)}_{fi}$:

$$T^{(1)}_{fi}=\langle\chi^-_f|W^\dagger_f|\chi^+_i\rangle\ , \tag{2.3}$$

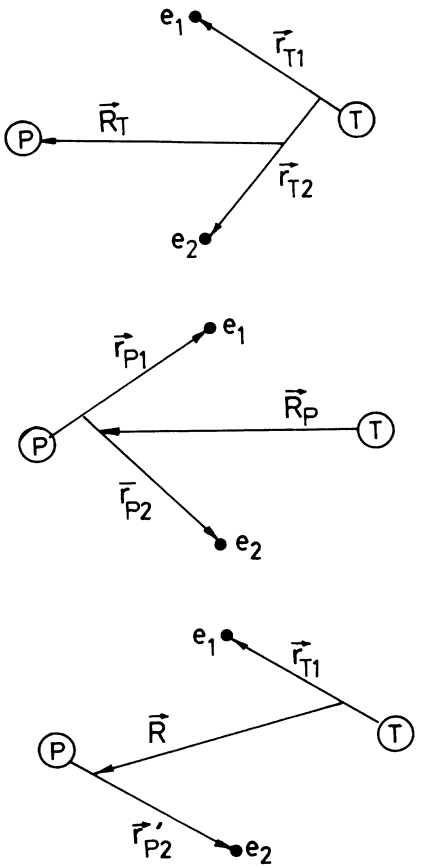

FIG. 1. Coordinate systems.

$$T^{(2)}_{fi}=\langle\chi^-_f|W^\dagger_f G^+ W_i|\chi^+_i\rangle\ , \tag{2.4}$$

G^+ being the total Green function. In Eq. (2.3) surface terms are considered to be null. χ^+_i and χ^-_f represent distorted-wave functions containing two electrons in the target and projectile, respectively, and they satisfy

$$(E-H\pm i\varepsilon)\chi^\pm_j=-W_j\chi^\pm_j,\quad j=i,f,\quad \varepsilon\to 0^+\ , \tag{2.5}$$

with E the total energy. The first order, $T^{(1)}_{fi}$ represents a mechanism where the two electrons jump together from the target to the projectile in a *single* step [10,14]. Crothers and McCarrol [10] calculated this term and concluded that it is negligible in comparison with the two-step mechanism (e.g., one order of magnitude smaller than the two-step process at 1.4 MeV of He^{2+} on He). Thus, we will not study this order and will concentrate only on the second one.

Replacing in Eq. (2.4) G^+ by G^+_N, which describes one electron in the target and the other in the projectile, we can approximate

$$T^{(2)}_{fi}=\sum_n\langle\chi^-_f|W^\dagger_f|\xi_n\rangle\frac{1}{E-E_n+i\varepsilon}\langle\xi_n|W_i|\chi^+_i\rangle\ , \tag{2.6}$$

where ξ_n are eigenfunctions of G^+_N, E_n is the eigenenergy, and the subindex n also involves the state of spin (which remains the same) and the continuum. The functions ξ_n should form a complete set, properly orthonormalized and symmetrized. Of course, as far as the bound electronic wave function is concerned, the nuclei are considered to have infinite masses.

The main approximation used to calculate the second order involves the consideration of only the on-shell contribution of Eq. (2.6), i.e.,

$$\frac{1}{E-E_n+i\varepsilon}=\mathrm{P}\left[\frac{1}{E-E_n}\right]-i\pi\delta(E-E_n)\ , \tag{2.7}$$

where the principal part (P) is neglected. With respect to this approximation, we point out the following: as shown by McGuire [15], the principal part plays an important role in double excitation when using Born wave functions [16]. But this is not the present case since we are going to use exact-impulse wave functions already containing the principal part of the corresponding propagators, and so the principal part in Eq. (2.7) is not expected to be very relevant. Anyway, the exact calculation of the complete second order, including the principle part, would involve a formidable numerical task, which we cannot face. The on-shell contribution, on the other hand provides a simple physical picture; i.e., the intermediate states satisfy the energy conservation. With this assumption, we can use the simplification introduced by the δ function. $T^{(2)}_{fi}$ then reads

$$T^{(2)}_{fi}=-\frac{i\pi}{v}\sum_n K_n^2\int_0^{2\pi}d\varphi_n\int_0^{\pi}d\theta_n\sin\theta_n T^-_{fn}T^+_{ni}\ , \tag{2.8}$$

where

$$K_n=\left[2\nu\left[\frac{K_i^2}{2\nu_T}+\epsilon_i-\epsilon_n\right]\right]^{1/2}\ , \tag{2.9}$$

where v is the impact velocity, θ_n is the angle between the initial momentum of the projectile $\mathbf{K}_i$, and the intermediate momentum $\mathbf{K}_n$, and φ_n is the azimuth angle. In Eq. (2.8)

$$T_{fn}^{-}=\langle\chi_f^{-}|W_f^{\dagger}|\xi_n\rangle,\quad T_{ni}^{+}=\langle\xi_n|W_i|\chi_i^{+}\rangle \tag{2.10}$$

correspond to transitions where one electron is captured and the other is relaxed to any state. In Eq. (2.9) ϵ_i and ϵ_n represent the initial and intermediate *two*- electron energy. No matter which distorted wave functions are employed, the contribution of this second order to the total cross section is found to be

$$\sigma^{(2)}=\frac{(2\pi)^6}{4v^4}\int d\boldsymbol{\eta}\left|\sum_n\int d\boldsymbol{\eta}_n T_{fn}^{-}(\boldsymbol{\eta}-\boldsymbol{\eta}_n)T_{ni}^{+}(\boldsymbol{\eta}_n)\right|^2, \tag{2.11}$$

where now the arguments of the T elements denote the corresponding transverse momenta

$$\begin{aligned}\boldsymbol{\eta}&=K_f\sin\theta(\cos\varphi,\sin\varphi,0)\ ,\\ \boldsymbol{\eta}_n&=K_n\sin\theta_n(\cos\varphi_n,\sin\varphi_n,0)\ .\end{aligned} \tag{2.12}$$

and K_f, θ and φ are the final momentum, polar angle, and azimuth angle of the rearrangement atom, respectively. Introducing the Fouier transforms

$$T_{ba}(\boldsymbol{\eta})=\frac{v}{(2\pi)^3}\int d\boldsymbol{\rho}a_{ba}(\boldsymbol{\rho})e^{-i\boldsymbol{\eta}\cdot\boldsymbol{\rho}}\ , \tag{2.13}$$

where ρ is the impact parameter, the total cross section reads

$$\sigma^{(2)}=\int d\boldsymbol{\rho}|\Lambda_{fi}(\boldsymbol{\rho})|^2\ , \tag{2.14}$$

where

$$\Lambda_{fi}(\boldsymbol{\rho})=\frac{i}{2}\sum_n a_{fn}^{-}(\boldsymbol{\rho})a_{ni}^{+}(\boldsymbol{\rho})\ . \tag{2.15}$$

Although the expression (2.14) does not seem to be familiar, the IEM is achieved by dropping $\sum_n$, considering frozen states (no relaxation), and neglecting correlation by replacing the transition amplitudes by the single-electron-capture ones. Further, as in most of the calculations, symmetric approximations are carried out to the point that a_{ba}^{+} is not distinguished from a_{ba}^{-}, as in the Brinkman-Kramers or continuum-distorted-wave (CDW) [6] approximations, and the well-known product of probabilities results.

The factor $i/2$ in Eq. (2.15) produces a coefficient 4^{-1} at level of the total cross section. It is partially or totally removed according to the symmetrization of the wave functions. At the level of T matrix, one may find interferences among the different "paths" that connect the initial $i=\{i_a,i_b\}$ with the final electronic state $f=\{f_c,f_d\}$ passing through the intermediate state $n=\{n_T,n_P\}$. Four possibilities can be identified where one electrons do the paths: $i_a\to n_T\to f_c$ and $i_b\to n_P\to f_d$; $i_a\to n_P\to f_c$ and $i_b\to n_T\to f_d$; $i_a\to n_P\to f_d$ and $i_b\to n_T\to f_c$; $i_a\to n_T\to f_d$ and $i_b\to n_P\to f_c$. In the particular case of $i_a=i_b$ and $f_c=f_d$, the four paths are equal and add coherently, thus, the 4^{-1} is totally removed. For a schematic picture, see Fig. 2: in the first step, one electron (say the active one) is captured and the other one (the passive one) is relaxed; in the second step the roles are exchanged.

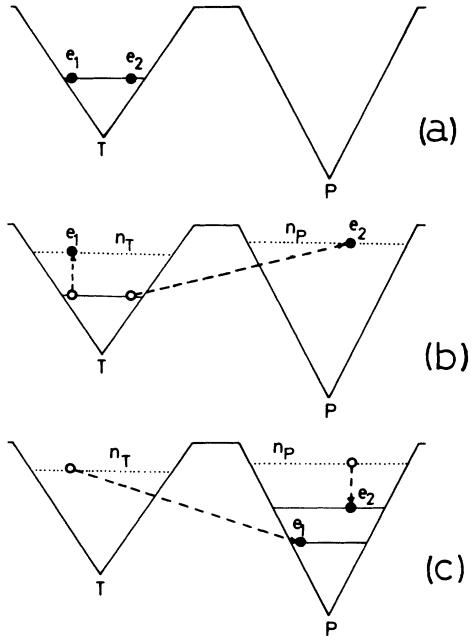

FIG. 2. Schematic picture for $1s^2\to 1s^2$ double capture. (a) Two electrons in the initial state. (b) The active electron (e_2) is captured to a state ϕ_{n_P} [of energy $-Z_P^2/(2n_P^2)$] and the passive one (e_1) relaxes to a state ϕ_{n_T} [of energy $-Z_T^2/(2n_T^2)$]. (c) The roles change. The active electron (e_1) is captured while e_2 relaxes to the final state.

III. THE EXACT-IMPULSE APPROXIMATION

Following the Coleman derivation [17], the initial *exact* two-electron impulse wave function reads

$$\begin{aligned}\chi_i^{I+}=&\frac{(1+P_{12})}{\sqrt{2}}\frac{1}{(2\pi)^{3/2}}\\ &\times\int d\mathbf{g}_1\int d\mathbf{g}_2\tilde{\phi}_{i_a}(\mathbf{g}_1)\tilde{\phi}_{i_b}(g_2)\psi_{\mathbf{g}_1-\mathbf{v}}^{P+}(\mathbf{r}_{P1})\psi_{\mathbf{g}_2-\mathbf{v}}^{P+}(\mathbf{r}_{P2})\\ &\times\exp[i(\mu_{T1}\mu_{T2}\mathbf{K}_i+\mathbf{g}_1+\mathbf{g}_2)\cdot\mathbf{R}_P]\ ,\end{aligned} \tag{3.1}$$

where

$$\psi_{\mathbf{k}}^{C\pm}(\mathbf{r})=\frac{1}{(2\pi)^{3/2}}e^{i\mathbf{k}\cdot\mathbf{r}}D^{\pm}(Z_c,\mathbf{k},\mathbf{r}),\quad C=T,P\ , \tag{3.2}$$

and for a pure Coulomb center

$$D^{\pm}(Z,\mathbf{k},\mathbf{r})=e^{(\pi/2)a}\Gamma(1\mp ia)_1F_1(\pm ia,1,\pm ikr-i\mathbf{k}\cdot\mathbf{r})\ , \tag{3.3}$$

with $a=Z/k$. Singlet states were considered. ϕ_α ($\alpha=i_a,i_b$) are the initial one-electron orbitals. The product $\phi_{i_a}(\mathbf{r}_{T1})\phi_{i_b}(\mathbf{r}_{T2})$ represents a term of a CI or HF ex-

pansion of the full initial electronic wave function $\Phi_i(\mathbf{r}_{T1},\mathbf{r}_{T2})$. The permutation operator P_{12} exchanges the electrons 1 and 2, and the tilde represents the Fourier transform.

It is clearly seen from Eq. (3.1) that the electrons are in the continuum of the projectile. Equivalently, for the final channel

$$\chi_f^{I-}=\frac{(1+P_{12})}{\sqrt{2}}\frac{1}{(2\pi)^{3/2}}\times\int d\mathbf{g}_1\int d\mathbf{g}_2\tilde{\phi}_{f_c}(\mathbf{g}_1)\tilde{\phi}_{f_d}(\mathbf{g}_2)\psi^{T-}_{\mathbf{g}_1+\mathbf{v}}(\mathbf{r}_{T1})\psi^{T-}_{\mathbf{g}_2+\mathbf{v}}(\mathbf{r}_{T2})\times\exp[i(\mu_{P1}\mu_{P2}\mathbf{K}_f-\mathbf{g}_1-\mathbf{g}_2)\cdot\mathbf{R}_T]\ , \tag{3.4}$$

where $\phi_\beta(\beta=f_c,f_d)$ are the final one-electron orbitals. Again, the product $\phi_{f_c}(\mathbf{r}_{P1})\phi_{f_d}(\mathbf{r}_{P2})$ represents a term of a CI or HF expansion of the full final electronic wave function $\Phi_f(\mathbf{r}_{P1},\mathbf{r}_{P2})$.

In the present paper we use exact-impulse wave functions to describe the initial and final states χ_i^{I+} and χ_f^{I-} as in Eqs. (3.1) and (3.4), and for the intermediate states we propose the following Born functions:

$$\xi_n=\frac{(1+P_{12})}{\sqrt{2}N_n}\xi_n'\ , \tag{3.5}$$

with

$$\xi_n'=\frac{1}{(2\pi)^{3/2}}e^{i\mathbf{K}_n\cdot\mathbf{R}}\phi_{n_T}(\mathbf{r}_{T1})\phi_{n_P}(\mathbf{r}'_{P2})\ , \tag{3.6}$$

where ϕ_{n_T} and ϕ_{n_P} are one-electron bound states in the target and in the projectile, respectively. The corresponding electronic energy ϵ_n is the sum of the individual electronic energies, and we assume the proposed set to satisfy the orthonormalization $N_n=1$.

As the T_{ni}^+ element is calculated on the energy-shell, we are able to use either W_i or the intermediate potential V_n [18], where $(H-E)\xi_n=V_n\xi_n$; then

$$T_{ni}^+=\langle\xi_n|W_i|\chi_i^{I+}\rangle=\langle\xi_n|V_n|\chi_i^{I+}\rangle=A_{ni}^{(1)+}+A_{ni}^{(2)+}+A_{ni}^{(3)+}\ , \tag{3.7}$$

where

$$A_{ni}^{(1)+}=\sqrt{2}\langle\xi_n'|V_{T2}|\chi_i^{I+}\rangle\ ,\quad A_{ni}^{(2)+}=\sqrt{2}\langle\xi_n'|V_{12}|\chi_i^{I+}\rangle\ ,\quad A_{ni}^{(3)+}=\sqrt{2}\langle\xi_n'|V_{P1}|\chi_i^{I+}\rangle\ . \tag{3.8}$$

The electronic repulsion is a *genuine* perturbation of the intermediate state, and since the electrons are in different centers, it decreases as the nuclei separate. We have

$$\begin{bmatrix}A_{ni}^{(1)+}\\A_{ni}^{(2)+}\end{bmatrix}=\frac{1}{(2\pi)^3}\int d\mathbf{g}_2\int d\mathbf{g}\,\tilde{\phi}_{i_b}(\mathbf{g}_2)L_{n_P}^{P+}(\mathbf{g}_2-\mathbf{v},\mathbf{U}_{P2}-\mathbf{g})\begin{bmatrix}\tilde{V}_{T2}(\mathbf{g}-\mathbf{g}_2) & C_{n_T,i_a}^{(1)+}(\mathbf{g})\\ \tilde{V}_{12}(\mathbf{g}_2-\mathbf{g}) & C_{n_T,i_a}^{(2)+}(\mathbf{g},\mathbf{g}_2)\end{bmatrix}+\mathrm{ch}(i_a\leftrightarrow i_b)\ ,$$
$$A_{ni}^{(3)+}=\frac{1}{(2\pi)^{3/2}}\int d\mathbf{g}_2\tilde{\phi}_{i_b}(\mathbf{g}_2)L_{n_P}^{P+}(\mathbf{g}_2-\mathbf{v},\mathbf{U}_{P2}-\mathbf{g}_2)C_{n_T,i_a}^{(3)+}(\mathbf{g}_2)+\mathrm{ch}(i_a\leftrightarrow i_b)\ , \tag{3.9}$$

where

$$\begin{bmatrix}C_{n_T,i_a}^{(1)+}(\mathbf{g})\\C_{n_T,i_a}^{(2)+}(\mathbf{g},\mathbf{g}_2)\end{bmatrix}=\int d\mathbf{g}_1\tilde{\phi}_{i_a}(\mathbf{g}_1)I^{P1+}(\mathbf{g}_1-\mathbf{v},\mathbf{U}_{P1}+\mathbf{g})\times\begin{bmatrix}\tilde{\phi}^*_{n_T}(\mathbf{U}_{T1}-\mathbf{g}_1-\mathbf{g})\\ \tilde{\phi}^*_{n_T}(\mathbf{U}_{T1}-\mathbf{g}_1-\mathbf{g}_2)\end{bmatrix}\ ,$$
$$C_{n_T,i_a}^{(3)+}(\mathbf{g}_2)=\int d\mathbf{g}_1\tilde{\phi}_{i_a}(\mathbf{g}_1)J^{P1+}(\mathbf{g}_1-\mathbf{v},\mathbf{U}_{P1}+\mathbf{g}_2)\times\tilde{\phi}^*_{n_T}(\mathbf{U}_{T1}-\mathbf{g}_1-\mathbf{g}_2)\ , \tag{3.10}$$

and

$$L_j^{C\pm}(\mathbf{k},\mathbf{q})=\frac{1}{(2\pi)^{3/2}}\int d\mathbf{r}\,e^{-i\mathbf{q}\cdot\mathbf{r}}D^{\pm}(Z_C,\mathbf{k},\mathbf{r})\phi_j^*(\mathbf{r}),$$
$$\begin{bmatrix}I^{C\pm}(\mathbf{k},\mathbf{q})\\J^{C\pm}(\mathbf{k},\mathbf{q})\end{bmatrix}=\frac{1}{(2\pi)^{3/2}}\int d\mathbf{r}\,e^{-i\mathbf{q}\cdot\mathbf{r}}D^{\pm}(Z_C,\mathbf{k},\mathbf{r})\times\begin{bmatrix}1\\V_C(\mathbf{r})\end{bmatrix},\quad C=T,P\ , \tag{3.11}$$

and the transfer momentum vectors U_{T1}, $\mathbf{U}_{P1}$, and $\mathbf{U}_{P2}$ are defined in the Appendix. In Eq. (3.9), $\mathrm{ch}(i_a\leftrightarrow i_b)$ means a similar term exchanging i_a with i_b.

Each first term of Eq. (3.9) can be physically described as follows: $A_{ni}^{(1)+}$ represents the capture of the electron e_2 (say active) by interaction with the projectile, while the electron e_1 (say passive) is relaxed by simple overlapping and it ends in the Coulomb field of the punctual charge Z_T. Since we are using the *exact* impulse approximation, the single-capture element $A_{ni}^{(1)+}$ includes multiple-scattering and Thomas processes. $A_{ni}^{(2)+}$ shows the same process involving the electronic repulsion. The last term $A_{ni}^{(3)+}$ describes the capture of e_2 via an interaction of the projectile with e_1, and this element is *null* in the impulse approximation because of the orthogonality between bound and continuum states of the projectile (in this case $L_{nP}^{P+}=0$). In all cases the second terms characterized by $\mathrm{ch}(i_c\leftrightarrow i_b)$ exchange roles.

The calculation is still very complex, since each term involves a nine-dimensional integral. A substantial simplification can be achieved if we replace the Coulomb interaction of the projectile with the passive electron by its asymptotic form. It is equivalent to approximate

$$D^{+}(Z_P,\mathbf{g}_1-\mathbf{v},\mathbf{r}_{P1})\sim\exp\left[-i\frac{Z_P}{v}\ln(vR_T-\mathbf{v}\cdot\mathbf{R}_T)\right] \tag{3.12}$$

in Eq. (3.10) to calculate I^{P1+}. Note that we still keep the full Coulomb interaction with the active electron. We drop the logarithmic phase factor in Eq. (3.12), which will be added to the one coming from the internuclear interaction in Sec. V. Afterwards, $C^{(1,2)+}_{n_T,i_a}$ reduces to

$$\begin{bmatrix} C^{(1)+}_{n_T,i_a}(\mathbf{g}) \\ C^{(2)+}_{n_T,i_a}(\mathbf{g},\mathbf{g}_2) \end{bmatrix}=(2\pi)^{3/2}\delta(\mathbf{g}+\mathbf{U}_{P1})\begin{bmatrix} K^{(1)+}_{n_T,i_a} \\ K^{(2)+}_{n_T,i_a} \end{bmatrix}, \tag{3.13}$$

with

$$K^{(1)+}_{n_T,i_a}=S_{n_T,i_a}(0),\quad K^{(2)+}_{n_T,i_a}=S_{n_T,i_a}(\mathbf{g}_2-\mathbf{U}_{T1}), \tag{3.14}$$

where

$$S_{\alpha,\beta}(\mathbf{u})=\int d\mathbf{r}\,\phi^{*}_{\alpha}(\mathbf{r})\phi_{\beta}(\mathbf{r})e^{i\mathbf{u}\cdot\mathbf{r}}, \tag{3.15}$$

having closed forms for any state. Then we arrive at

$$\begin{bmatrix} A^{(1)+}_{ni} \\ A^{(2)+}_{ni} \end{bmatrix}=\frac{1}{(2\pi)^{3/2}}\int d\mathbf{g}_2\tilde{\phi}_{i_b}(\mathbf{g}_2)L^{P+}_{n_P}(g_2-\mathbf{v},\mathbf{U}_{P2}+\mathbf{U}_{P1})\times\begin{bmatrix} \tilde{V}_{T2}(-\mathbf{g}_2-\mathbf{U}_{P1}) & K^{(1)+}_{n_T,i_a} \\ \tilde{V}_{12}(\mathbf{g}_2+\mathbf{U}_{P1}) & K^{(2)+}_{n_T,i_a} \end{bmatrix}+\mathrm{ch}(i_a\leftrightarrow i_b). \tag{3.16}$$

In similar fashion, we find that

$$T^{-}_{fn}=\langle\chi^{I-}_f|W^{\dagger}_f|\xi_n\rangle=A^{(1)-}_{fn}+A^{(2)-}_{fn}, \tag{3.17}$$

with

$$\begin{bmatrix} A^{(1)-}_{fn} \\ A^{(2)-}_{fn} \end{bmatrix}=\frac{1}{(2\pi)^{3/2}}\int d\mathbf{g}_1\tilde{\phi}^{*}_{f_c}(-\mathbf{g}_1)L^{T-*}_{n_T}(\mathbf{g}_1+\mathbf{v},-\mathbf{P}_{T1})\times\begin{bmatrix} V_{P1}(\mathbf{g}_1+\mathbf{P}_{P1}) & K^{(1)-}_{f_d,n_P} \\ \tilde{V}_{12}(\mathbf{g}_1+\mathbf{P}_{P1}) & K^{(2)-}_{f_d,n_P} \end{bmatrix}+\mathrm{ch}(f_c\leftrightarrow f_d), \tag{3.18}$$

where

$$K^{(1)-}_{f_d,n_P}=S_{f_d,n_P}(0),\qquad K^{(2)-}_{f_d,n_P}=S_{f_d,n_P}(-\mathbf{g}_1-\mathbf{P}_{P1}), \tag{3.19}$$

and the transfer momentum vectors $\mathbf{P}_{T1},\mathbf{P}_{P1}$ are defined in the Appendix.

$K^{(1)\pm}_{\alpha,\beta}$ are simple relaxation factors, while $K^{(2)\pm}_{\alpha,\beta}$ are relaxation functions depending on the variable of integration. In Eqs. (3.16) and (3.18), $A^{(1)+}_{ni}$ and $A^{(1)-}_{fn}$ are found to be the sum of the exact-impulse-approximation T-matrix elements of single capture times the relaxation factors $K^{(1)\pm}_{\alpha,\beta}$. $A^{(2)+}_{ni}$ and $A^{(2)-}_{fn}$ represent the contribution of the capture process involving the electron-electron repulsion, and they include within the integration the relaxation functions $K^{(2)\pm}_{\alpha,\beta}$. Besides the relaxation, the presence of $A^{(2)+}_{ni}$ and $A^{(2)-}_{fn}$ differentiates this calculation from the IEM.

Finally, using Eq. (2.8), we write the T matrix as follows:

$$T^{(2)}_{fi}=-\frac{i\pi}{v}\sum_n\int d\eta_n(A^{(1)-}_{fn}+A^{(2)-}_{fn})(A^{(1)+}_{ni}+A^{(2)+}_{ni}). \tag{3.20}$$

IV. TOTAL CROSS SECTIONS

To obtain a second-order total cross section, five-dimensional integrals are required: three-dimensional ones to obtain $T^{\pm}_{ba}$, another one to obtain $a^{\pm}_{ba}(\rho)$, and a final one on the impact parameters. Alternatively, with the T-matrix elements, Eq. (2.11) can be integrated directly. Numerical errors are estimated to be around 3% at most.

A. Resonant symmetric collisions

To study the symmetric and resonant reaction

$$\mathrm{He}^{2+}+\mathrm{He}(1s^2)\rightarrow\mathrm{He}(1s^2)+\mathrm{He}^{2+}, \tag{4.1}$$

we have used two descriptions of the electronic ground state, namely CI and HF Clementi-Roetti [19] wave functions.

1. Use of CI wave functions

We construct the following CI to describe the ground state of helium:

$$|\Phi^{(\mathrm{CI})}\rangle=(0.9327|\Phi_1\rangle-0.3536|\Phi_2\rangle-0.0339|\Phi_3\rangle-0.0619|\Phi_4\rangle)\otimes|S=0,M_S=0\rangle, \tag{4.2}$$

where

$$\begin{aligned}
|\Phi_1\rangle&=|1s^2\rangle=|\phi_{1s},\phi_{1s}\rangle,\\
|\Phi_2\rangle&=|1s,2s\rangle=\frac{1}{\sqrt{2}}(|\phi_{1s},\phi_{2s}\rangle+|\phi_{2s},\phi_{1s}\rangle),\\
|\Phi_3\rangle&=|1s,3s\rangle=\frac{1}{\sqrt{2}}(|\phi_{1s},\phi_{3s}\rangle+|\phi_{3s},\phi_{1s}\rangle),\\
|\Phi_4\rangle&=|2p,2p\rangle=\frac{1}{\sqrt{3}}(|\phi_{2p0},\phi_{2p0}\rangle-|\phi_{2p1},\phi_{2p-1}\rangle-|\phi_{2p-1},\phi_{2p1}\rangle).
\end{aligned} \tag{4.3}$$

The r representation of a ket of the basis is $\langle\mathbf{r}_1,\mathbf{r}_2|\phi_{nlm},\phi_{n'l'm'}\rangle=\phi_{nlm}(\mathbf{r}_1)\phi_{n'l'm'}(\mathbf{r}_2)$. The radial part of $\phi_{nlm}(\mathbf{r})$, namely $R_{nl}(r)$, is expressed in terms of the Slater orbitals $S_{nl}(Z|r)$, where Z is the exponential coefficient or effective charge. We find the following expressions:

$$
\begin{aligned}
R_{1s}(r)&=S_{1s}(2.153|r)\ ,\\
R_{2s}(r)&=0.3992S_{1s}(2.153|r)+1.331S_{1s}(1.034|r)-2.305S_{2s}(1.424|r)\ ,\\
R_{3s}(r)&=0.4275S_{1s}(2.153|r)+1.312S_{1s}(1.034|r)-2.272S_{2s}(1.424|r)\\
&\quad+1.991S_{1s}(0.4738|r)-6.896S_{2s}(0.6342|r)+6.295S_{3s}(0.9154|r)\ ,\\
R_{2p}(r)&=S_{2p}(2.451|r)\ .
\end{aligned}
\tag{4.4}
$$

The present CI wave function has a similar structure to the one used by Fritsch and Lin [12] but here the charges of the Slater orbitals were optimized, minimizing the energy by using the ATMOLCI program [20]. The energy of our CI wave function is -2.873, being slightly better than the energy of the HF function (-2.862) [19]. Because the number of elements $A_{ab}^{(1,2)\pm}$ to be calculated is proportional to the number of Slater orbitals, and considering that each of those elements involves a three-dimensional integral, we should be able to accurately describe the electronic states. The total cross section for the reaction (4.1) is displayed in Fig. 3 along with the experiments of McDaniel *et al.* [21], DuBois [22], and Castro Faria, Freire, and de Pinho [23]. The intermediate states were assumed to be only ground states around each center. The agreement with the data is very good.

2. *Use of HF wave functions*

In particular, we have used the 5-z HF Clementi-Roetti [19] wave function to describe the electronic ground state of helium. We have considered as intermediate states only $1s$ states around each center, and it has been found that $K^{(1)\pm}=0.982$, indicating that relaxation to high intermediate states ($n_T,n_P\geq 2$) represents less than 4% in each center. For reaction (4.1), we have found that the difference between the results using HF and CI wave functions is *less* than the numerical uncertainty of 3%. Taking into account the limitation of the CI wave function used, it is found that correlation in the ground state (the so-called static correlation) does not seem to be relevant, at least for the present case. Note that in our formalism the electronic repulsion is considered as a first-order perturbation during the collision (the so-called dynamic correlation). Hereafter, we use HF wave functions to calculate the next reactions involving capture to ground and single excited states. However, if we dealt with double excited states, we would certainly be forced to use very precise CI functions.

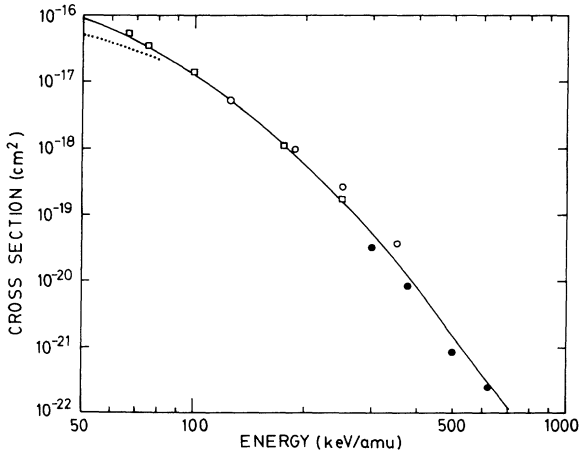

FIG. 3. $1s^2\rightarrow 1s^2$ double-electron-capture cross sections for He^{2+}-He collision. The data involve capture to all states. Solid line, second-order impulse approximation as calculated in Sec. IV A using the CI wave function; dotted line, close-coupling calculation using a Gauss-type expansion from Gramlich, Grün, and Scheid [13]. ○, experiments from McDaniel *et al.* [21]; □, experiments from DuBois [22]; ●, experiments from Castro Faria, Freire, and de Pinho [23].

In Table I we compare our results with those of Crothers and McCarroll [10] (column C-Mc) calculated with the Pluvinage electronic wave function, which includes correlation. Even though the theoretical methods are different, the similarity of the values is a new indication that the use of HF orbitals is appropriate.

We also display the results of Gayet, Rivarola, and Salin [6] calculated with the CDW within the IEM and using the same HF bound state without (column IEM-CDW) [case (i)] and with (column IEM-CDW) [case (ii)] relaxation. At this point it is interesting to compare our calculations within the IEM using the *same* method, i.e., the exact-impulse approximation. To this end, we have calculated exact-impulse amplitudes corresponding to a one-electron system and we have proceeded as in case (i) of Gayet, Rivarola, and Salin [6]. The results shown in the table (column IEM-IA) are very similar to those of the IEM-CDW [case (i)] [6]. The differences between the IEM and the two-electron model considered here lie in the presence of the term $1/r_{12}$ (sometime called dynamic correlation) as an active perturbation, and not in the use of elaborated initial electronic wave functions (static correlation), such as the use of CI.

The high-energy limit was roughly fitted to be v^{-20} in the velocity range 10–15, in agreement with the result of McGuire [24]. It may be an indication that the shake-over process is included through the terms $A_{fn}^{(2)-}A_{ni}^{(1)+}$ and $A_{fn}^{(1)-}A_{ni}^{(2)+}$. We do not know whether the high-energy limit has been reached at these velocities. It should be noted that by using IEM amplitudes and neglecting all double-scattering terms (those leading to v^{-11} in single capture), the cross section should tend to $Z_T^{10}Z_p^{10}v^{-22}$ [24,14].

B. Nonresonant symmetric collisions

We are interested in the following double-capture process:

TABLE I. $1s^2 \rightarrow 1s^2$ double-electron-capture cross sections (in cm^2) for He^{2+}-He collisions. E is the projectile impact energy (in keV). Experiments are taken from McDaniel *et al.* [21], involving capture to all the states: IEM-CDW, independent-electron-model results with the CDW as reported by Gayet, Rivarola, and Salin [6] without (i) and with (ii) relaxation, respectively; IEM-IA, independent-electron-model results with the exact-impulse approximation using the HF single-z wave function (see text); C-Mc, the best calculations of Crothers and McCarroll [10] with Pluvinage electronic wave functions within the CDW approximation; this work, the second order with the impulse approximation as calculated in Sec. IV A using HF wave functions. The use of CI wave functions gives the same results within the two significant figures.

E (keV)	Experiment	IEM-CDW	IEM-IA	C-Mc	This work
500	5.1×10^{-18}	16×10^{-18} (i) 13×10^{-18} (ii)	13×10^{-18}	5.8×10^{-18}	5.0×10^{-18}
750	9.5×10^{-19}	18×10^{-19} (i) 11×10^{-19} (ii)	18×10^{-19}	7.4×10^{-19}	7.6×10^{-19}
1000	2.6×10^{-19}	3.1×10^{-19} (i) 1.7×10^{-19} (ii)	3.4×10^{-19}	1.5×10^{-19}	1.6×10^{-19}
1400	3.6×10^{-20}	3.4×10^{-20} (i) 1.7×10^{-20} (ii)	3.7×10^{-20}	2.1×10^{-20}	1.9×10^{-20}

$$He^{2+}+He(1s^2)\rightarrow He(1s^2,1s2s,1s2p)+He^{2+} . \quad (4.5)$$

We will here concentrate on 180 keV impact energy where experiments are available. Obviously, the singlet state is considered. The initial bound state was again represented by the 5-z Clementi-Roetti wave function [19], and the final ones were described by variational wave functions [25]. State-to-state total cross sections were calculated to be 5.7, 1.8, and 0.97×10^{-17} cm^2 for $1s^2\rightarrow1s^2$, $1s^2\rightarrow1s2s$, and $1s^2\rightarrow1s2p$, respectively. It makes a total cross section of 8.5×10^{-17} cm^2, which compares reasonably well with the experimental value [26] (around 6.20×10^{-17} cm^2).

For the present case, we have studied the influence of the intermediate states. For $1s^2\rightarrow1s2s$ double capture we found that the main contribution comes from the intermediate states ($n_T=1s$, $n_P=2s$) and ($n_T=1s$, $n_P=1s$); *individual* contributions [27] were found to be 4.5 and 4.6×10^{-18} cm^2, respectively. Other intermediate states such as ($n_T=2s$, $n_P=1s$) and ($n_T=2s$, $n_P=2s$) were found to be of the order of a few percent. For $1s^2\rightarrow1s2p$ we analyzed the influence of five intermediate states including the $n=1$ shell around the target and $n=1,2$ shells around the projectile. Similarly, we found that ($n_T=1s$, $n_P=2p$) and ($n_T=1s$, $n_P=1s$) are dominant. Again, contributions from other intermediate states were found to be small. We conclude that for the present system the most relevant intermediate states are those corresponding to the final state, and other states can be neglected, as we did in the previous section.

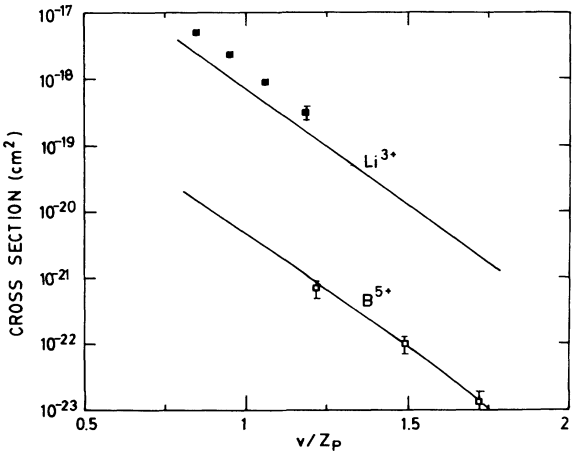

FIG. 4. $1s^2\rightarrow1s^2$ double-electron capture by Li^{3+} and B^{5+} on helium targets as a function of the ion velocity normalized to Z_P. The data involve capture to all states. Solid line, the present theory as calculated in Sec. IV C; ■, experiments from Shah and Gilbody [28]; □, experiments from Hippler *et al.* [29].

C. Asymmetric collisions

Figure 4 shows double capture of multicharged ions on helium:

$$X^{Z+}+He(1s^2)\rightarrow X^{(Z-2)+}(1s^2)+He^{++} , \quad (4.6)$$

and compared with the available experiments [28,29]. For the initial electronic orbital, we have used the 5-z HF Clementi-Roetti wave function [19], while for the final one we have used the 3-z HF function for the He(^{1}S) isoelectronic series [19]. In general, our theory follows the experiments. For B^{5+} impact, the agreement with the data is better than expected if we consider that we have not taken into account capture to excited states, which would increase the cross section. On the contrary, such an increment would improve the Li^{3+} results.

V. DIFFERENTIAL CROSS SECTIONS

The differential cross section is simply

$$\frac{d\sigma^{(2)}}{d\Omega}=\frac{K_f^2}{(2\pi)^2}\left|\int d\rho\,\rho^{i2\lambda}\Lambda_{if}(\rho)e^{-i\eta\cdot\rho}\right|^2 , \quad (5.1)$$

where λ is the Coulomb parameter of internuclear interaction. In principle, λ should be Z_TZ_P/v; however, to

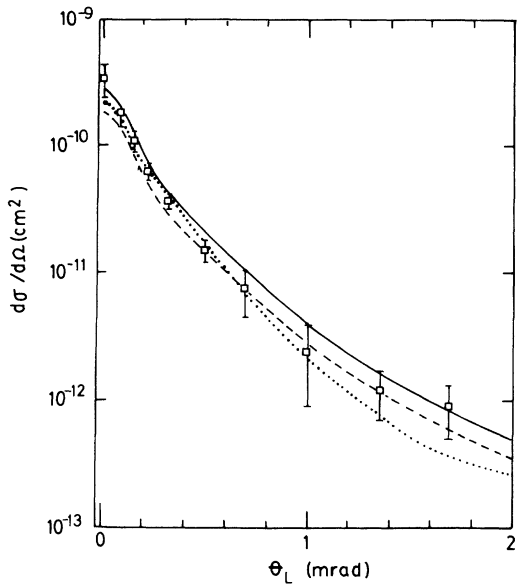

FIG. 5. Differential cross section for double-capture $^3He^{2+}+^4He(1s^2)$ involving capture to $1s^2$, $1s2s$, and $1s2p$ states for 60 keV/amu impact energy. The data involve capture to all states. Dashed and solid lines, $1s^2\rightarrow 1s^2$ and total differential cross section calculated with the second-order impulse approximation, respectively; dotted line, classical trajectory Monte Carlo calculation from Meng and Reinhold [26]; □, experiments from Irby *et al.* [30].

be consistent with our approximation [see Eq. (3.12)], we have to rest the asymptotic phase of the passive electron, giving $\lambda=(Z_T-1)Z_P/v$. The differential cross section is plotted in Fig. 5 for the symmetric case $^3He^{2+}+^4He(1s^2)$ involving capture to $1s^2$, $1s2s$, and $1s2p$ states for 60 keV/amu impact energy. The present theory compares well not only with the experiments [30] but also with the classical trajectory Monte Carlo calculations [26].

It should be noted that we are dealing with a symmetric case where $Z_T=Z_P=2$. In this case, the Coulomb parameter in the initial channel is equal to that of the final one: i.e., $(Z_T-1)Z_P/v=Z_T(Z_P-1)/v=2/v$, therefore we can build up a common value λ. However, in an asymmetric case, the use of a unique parameter is not evident. This problem would be solved by keeping the phase factor of the passive electron in Eq. (3.12) throughout the calculation.

VI. CONCLUSIONS

Double capture has been studied as a second order in the distorted-wave formalism. This second order represents the double process as two subsequent single-capture processes involving also relaxation and the intermediate cascade, and it was calculated with the exact-impulse approximation. Within this formalism and for $1s^2\rightarrow 1s^2$ double capture, we find that there are not appreciable differences between the use of CI and HF wave functions to represent the electronic state.

Some improvements could be made in our calculations: (i) there should be improvement of the intermediate states to account for the distortion of the Coulomb charges, for example via eikonals, instead of the simple Born wave functions. (ii) The calculations should account for the full distortion of the passive electron during the collision. Within our formalism, this means to giving an exact expression for the factors $C^{(1,2)\pm}_{\alpha,\beta}$. Unfortunately, this it would necessitate a much more detailed calculation than the present one. (iii) It would be beneficial to also calculate the principal part neglected in our calculation [see Eq. (2.7)]. The task is very difficult, and would be prohibitive for our present computing system.

Capture to double excited states can also be calculated with this formalism; however, special attention should be paid to the description of the final state. Although we apply this formalism to double capture, it is evident that it can be extended to other double processes such as capture and excitation, capture and ionization, double excitation, etc. Further, to treat multiple processes, we should resort to higher perturbation orders; e.g., for triple capture, we should deal with the third order.

ACKNOWLEDGMENTS

We would like to thank J. McGuire and A. Salin for fruitful discussions. We are indebted to Professor Bunge for implementing his ATMOLCI program in our computer system. We also thank L. Meng and C. O. Reinhold for providing us with the angular distribution data prior to publication.

APPENDIX

The transformation formulas are, for any masses (see Fig. 2),

$$\begin{aligned}
\mathbf{R}_T&=\frac{M_T}{(M_T+2)}\mathbf{R}_P-\frac{M_T+M_P+2}{(M_T+2)(M_P+1)}\mathbf{r}_{P1}\\
&\quad-\frac{M_T+M_P+2}{(M_T+2)(M_P+2)}\mathbf{r}_{P2}\,,\\
\mathbf{r}_{T1}&=\mathbf{R}_P+\frac{M_P}{M_P+1}\mathbf{r}_{P1}-\frac{1}{M_P+2}\mathbf{r}_{P2}\,,\\
\mathbf{r}_{T2}&=\frac{M_T}{M_T+1}\mathbf{R}_P-\frac{M_P}{(M_T+1)(M_P+1)}\mathbf{r}_{P1}\\
&\quad+\frac{1+(M_T+1)(M_P+1)}{(M_T+1)(M_P+2)}\mathbf{r}_{P2}\,,
\end{aligned}\tag{A1}$$

and

$$\begin{aligned}
\mathbf{R}&=\frac{M_T}{M_T+1}\mathbf{R}_P-\frac{M_P(M_T+M_P+2)}{(M_T+1)(M_P+1)^2}\mathbf{r}_{P1}\\
&\quad+\frac{M_T+M_P+2}{(M_T+1)(M_P+1)(M_P+2)}\mathbf{r}_{P2}\,,\\
\mathbf{r}_{T1}&=\mathbf{R}_P+\frac{M_P}{M_P+1}\mathbf{r}_{P1}-\frac{1}{M_P+2}\mathbf{r}_{P2}\,,\\
\mathbf{r}'_{P2}&=\frac{1}{M_P+1}\mathbf{r}_{P1}+\mathbf{r}_{P2}\,,
\end{aligned}\tag{A2}$$

and another relation can be easily obtained from these.

The transfer momentum vectors can be defined by

$$\mathbf{K}_i\cdot\mathbf{R}_T-\mathbf{K}_n\cdot\mathbf{R}=-\mathbf{U}_{T1}\cdot\mathbf{r}_{T1}-\mathbf{U}_{P1}\cdot\mathbf{r}_{P1}-\mathbf{U}_{P2}\cdot\mathbf{r}_{P2}\ , \tag{A3}$$

$$\mathbf{K}_n\cdot\mathbf{R}-\mathbf{K}_f\cdot\mathbf{R}_P=-\mathbf{P}_{T1}\cdot\mathbf{r}_{T1}-\mathbf{P}_{P1}\cdot\mathbf{r}_{P1}-\mathbf{P}_{P2}\cdot\mathbf{r}_{P2}\ . \tag{A4}$$

For heavy nuclei, using energy conservation, these vectors read

$$\begin{aligned}\mathbf{U}_{T1}&=\boldsymbol{\eta}_n+\left[\frac{v}{2}+\frac{(\epsilon_i-\epsilon_n)}{v}\right]\hat{\mathbf{z}}\ ,\\ \mathbf{U}_{P1}&=-\boldsymbol{\eta}_n-\left[\frac{v}{2}+\frac{(\epsilon_i-\epsilon_n)}{v}\right]\hat{\mathbf{z}}\ ,\\ \mathbf{U}_{P2}&=v\hat{\mathbf{z}}\ ,\end{aligned} \tag{A5}$$

$$\begin{aligned}\mathbf{P}_{T1}&=\boldsymbol{\eta}-\boldsymbol{\eta}_n+\left[\frac{v}{2}+\frac{(\epsilon_n-\epsilon_f)}{v}\right]\hat{\mathbf{z}}\ ,\\ \mathbf{P}_{P1}&=-\boldsymbol{\eta}+\boldsymbol{\eta}_n+\left[\frac{v}{2}-\frac{(\epsilon_n-\epsilon_f)}{v}\right]\hat{\mathbf{z}}\ ,\\ \mathbf{P}_{P2}&=0\ ,\end{aligned} \tag{A6}$$

where $\epsilon_{i,f,n}$ are the initial, final, and intermediate two-electron binding energies, the z axis was chosen to be along the velocity, and $\boldsymbol{\eta}$ and $\boldsymbol{\eta}_n$ are the transversal momenta given by

$$\begin{aligned}\boldsymbol{\eta}&=K_f\sin\theta(\cos\varphi,\sin\varphi,0)\ ,\\ \boldsymbol{\eta}_n&=K_n\sin\theta_n(\cos\varphi_n,\sin\varphi_n,0)\ .\end{aligned} \tag{A7}$$

[1] T. J. M. Zourus, D. Schneider, and N. Stolterfoht, Phys. Rev. A **35**, 1963 (1987).

[2] J. H. McGuire and L. Weaver, Phys. Rev. A **16**, 41 (1977).

[3] Dz. Belkić, R. Gayet, and A. Salin, Phys. Rep. **56**, 279 (1979).

[4] M. Mittleman, Phys. Rev. **137**, A1 (1965).

[5] T. C. Theisen and J. H. McGuire, Phys. Rev. A **20**, 1406 (1979).

[6] R. Gayet, R. D. Rivarola, and A. Salin, J. Phys. B **14**, 2421 (1981).

[7] M. Ghosh, C. R. Mandal, and S. C. Mukherjee, Phys. Rev. A **35**, 5259 (1987).

[8] S. N. Chatterjee and B. N. Roy, J. Phys. B **18**, 4283 (1985).

[9] R. E. Olson, J. Phys. B **15**, L163 (1982).

[10] D. S. F. Crothers and R. McCarroll, J. Phys. B **20**, 2835 (1987).

[11] W. Fritsch and C. D. Lin, J. Phys. B **19**, 2683 (1986).

[12] W. Fritsch and C. D. Lin, Phys. Rev. A **41**, 4776 (1990).

[13] K. Gramlich, N. Grün, and W. Scheid, J. Phys. B **22**, 2567 (1989).

[14] J. E. Miraglia and M. S. Gravielle, in *Abstracts of Contributed Papers to the 15th International Conference on the Physics of Electronic and Atomic Collisions, Brighton, 1987,* edited by J. Geddes *et al.* (North-Holland, Amsterdam, 1987), p. 521.

[15] J. McGuire (private communcation).

[16] When using unperturbed Born wave functions in double excitation, $T_{fi}^{(1)}$ is real and proportional to Z_P, and the principal part also being real contributes to the Z_P^3 terms of the cross section. Since the energy conservation is imaginary, it gives a contribution of the order of Z_P^4 and is therefore less important than the principal part.

[17] J. P. Coleman, in *Case Studies in Atomic Collision Physics I,* edited by E. W. McDaniel and M. C. R. McDowell (North-Holland, Amsterdam, 1969), p. 101.

[18] We note that $\langle\xi_n|W_i|\chi_i^+\rangle=\langle\xi_n|H-E|\chi_i^+\rangle=\langle\xi_n|E_n-E+V_n|\chi_i^+\rangle$, where E_n is the energy of the intermediate state ξ_n. Since we are working on-shell, $E=E_n$ [see Eq. (2.7)].

[19] E. Clementi and C. Roetti, At. Data Nucl. Data Tables **14**, 177 (1974).

[20] A. V. Bunge, C. F. Bunge, R. Jáuregui, and G. Cisneros, Comput. Chem. **13**, 201 (1989); C. F. Bunge, R. Jáuregui, and G. Cisneros, *ibid.* **13**, 277 (1989).

[21] E. W. McDaniel, M. R. Flannery, H. W. Ellis, F. L. Eisele, and W. Pope, U.S. Army Missile Research and Development Command Technical Report No. H 78-1, 1977 (unpublished).

[22] R. D. DuBois, Phys. Rev. A **36**, 2585 (1987).

[23] N. V. de Castro Faria, F. L. Freire, Jr., and A. G. de Pinho, Phys. Rev. A **37**, 280 (1988).

[24] J. H. McGuire, N. C. Deb, Y. Aktas, and N. C. Sil, Phys. Rev. A **38**, 3333 (1988).

[25] W. Fritsch and C. D. Lin, Phys. Rev. Lett. **61**, 690 (1988).

[26] L. Meng and C. O. Reinhold (private communication).

[27] Note that each contribution should be added coherently.

[28] M. B. Shah and H. B. Gilbody, J. Phys. B **18**, 899 (1985).

[29] R. Hippler, S. Datz, P. D. Miller, P. L. Pepmiller, and P. F. Dittner, Phys. Rev. A **35**, 585 (1987).

[30] V. Irby *et al.* (unpublished). Results provided by C. Reinhold in Ref. [26].